Mikael Ögren

# Propagation of Sound – Screening and Ground Effect Part 1: Non-Refracting Atmosphere

SP Swedish National Testing and Research Institute
Acoustics
SP REPORT 1997:44

# Abstract

This report presents an evaluation of several published theoretical models for the calculation of sound propagation in a non-refracting atmosphere. The models are described in detail and have been implemented and tested. The evaluation did not focus on the theoretical foundations of the models, but rather on the calculation performance and the accuracy as compared to measurements and reference cases solved by other methods. No numerical methods like FEM or BEM have been included in the studies, since they are too slow to be used in general noise prediction models because they require too complex input data.

Chapter 2 deals with widely used solutions for ground effect, which have been shown to agree well with measured results and experience. Chapter 3 and 4 deal with diffraction models, and they have been evaluated with respect to their speed of calculation, accuracy and adaptability to different situations. Finally, chapter 5 presents results of multiple diffraction models, for cases such as multiple screens and wide barriers. In the annexes A and B model measurements are presented for the wide and double screen cases.



Key words: acoustics, propagation, screens, wide barriers, noise prediction



**SP Sveriges Provnings- och Forskningsinstitut**
SP Rapport 1997:44
ISBN 91-7848-713-7
ISSN 0284-5172
Borås 1998


felaktigt!


**SP Swedish National Testing and Research Institute**
SP Report 1997:44



**Postal address:**
**Box 857, S-501 15 BORÅS**
**Sweden**
**Telephone +46 33 16 50 00**
**Telex 36252 Testing S**
**Telefax 46 33 13 55 02**

# Contents

# Preface

This project has been funded by the Nordic Ministry of Councils, through the Environmental Noise 2000 project, and by KFB, the Swedish Transport and Communications Research Board, project 1997-0225.

I would like to express my gratitude towards Lars Larsson, who made the model measurements, and to Hans Jonasson, Birger Plovsing and Tomas Ström for their support and resourcefulness.

# Conclusions

This report presents an evaluation of a number of theoretical models, taken from research articles, concerning calculation of sound propagation in a non-refracting atmosphere. The models have been presented in detail, and evaluated with respect to their accuracy, calculation speed and adaptability to different situations.

For the plane ground effect, the spherical wave reflection coefficient introduced by Ingard is a very good solution. It has been proven to be accurate, and it is very fast compared to numerical solutions. For the calculation of diffraction the model by Hadden/Pierce is the most versatile and accurate solution, since it can be modified to deal with impedance surfaces. To combine diffraction and ground effect, the image model introduced by Jonasson has proven to be fast and accurate. Finally, for multiple diffraction, such as wide screens, the model proposed by Salomons gives acceptable results for the tested geometries.

# 1 Introduction

## 1.1 List of symbols

| | |
|---|---|
| $a_1, a_2$ | Size of the Fresnel-zone [m] |
| c | Speed of sound , in the examples c=340 m/s is assumed [m/s] |
| d | Horizontal distance between source and receiver [m] |
| $d_S$ | Horizontal distance between source and screen [m] |
| $d_R$ | Horizontal distance between screen and receiver [m] |
| f | Frequency [Hz] |
| f(x),g(x) | Auxiliary Fresnel functions, see (3.5) |
| F(x) | The Fresnel integral, see (3.1) |
| $h_R$ | Receiver height above the ground [m] |
| $h_S$ | Source height above the ground [m] |
| $h_{SC}$ | Screen height above the ground [m] |
| H(x) | The Heaviside step function |
| k | Wavenumber, $k=\omega/c$ [$m^{-1}$] |
| **n** | Normal vector into the ground surface [-] |
| p | Acoustic pressure [Pa] |
| Q | Spherical reflection coefficient [-] |
| R | Plane wave reflection coefficient [-] |
| $R_n$ | Length of ray number n [m] |
| t | Time [s] |
| **v** | Acoustic velocity vector [m/s] |
| $x_{SRP}$ | Point of specular reflection, measured from the source [m] |
| Z | Specific normalized acoustic impedance [Pa s / m] |
| $\beta$ | Exterior wedge angle [rad] |
| $\nu$ | Normalized admittance [m/Pa s] or wedge index $\nu=\pi/\beta$ [-] |
| $\omega$ | Angular frequency ($\omega=2\pi f$) [rad/s] |
| $\sigma$ | The effective flow resistivity [$Nsm^{-4}$] |

# 2 Ground effect on sound propagation

The ground effect in sound propagation is determined by the impedance of the ground and by the geometrical situation. The effect is strongly frequency dependent. If you consider a point source over an infinitely rigid boundary, you will in principle get two sound rays, one direct and one reflected. These two rays interfere, and cause dips in the frequency response where the difference in traveled distance is $n\lambda+\lambda/2$, n=0,1,2.... When we have a boundary with a specific acoustic impedance, the reflected ray is affected both in amplitude and in phase, which changes the location of the frequency dips, and the overall frequency response.

## 2.1 Acoustic impedance

### 2.1.1 Definition of specific acoustic impedance

The specific acoustic (surface) impedance (called impedance from now on) is defined as the complex ratio of the effective sound pressure at a point of an acoustic medium to the effective particle velocity normal to the surface (positive direction into the surface) at that point. The SI unit is $Ns/m^3$. The word "specific" implies "per unit area", since pressure is force per unit area.

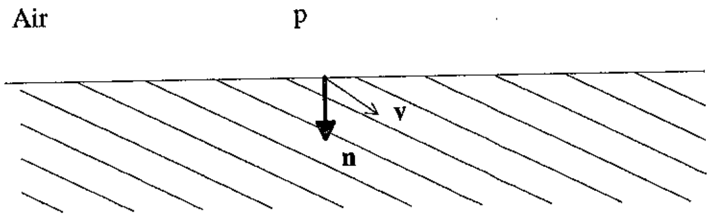


*Figure 2.1 Definition of specific acoustic impedance.*

$$Z(\omega) = \frac{\hat{p}}{\hat{\mathbf{v}} \bullet \mathbf{n}} \tag{2.1}$$

The admittance, in the following denoted $\nu$, is the inverse of the impedance. The real part of the impedance is called resistance and the imaginary reactance. If the time dependence is described as $e^{i\omega t}$ instead of $e^{-i\omega t}$, the reactance would have the opposite sign of what the definition here would give. In other words, the impedance will be conjugated if the time dependence changes sign.

To characterize a surface it is usual to state the surface impedance normalized to the impedance of air, $Z_{norm}=Z/\rho_0 c$, where $\rho_0$ is the density of air, and c the speed of sound. In the following text the normalized specific acoustic impedance is referred to as impedance.

### 2.1.2 Local and extended reaction

A surface is called locally reacting if the particle velocity (**v•n**) at a point depends only on the pressure p at the same point. If this is not the case, the surface is called extendedly reacting. The assumption that a surface is locally reacting is the same as to assume that the impedance of the surface is independent of the angle of incidence. There is no evidence that suggests that normal ground surfaces can not be classified as locally reacting. Some very soft surfaces, like snow, are not locally reacting, but can usually be analyzed as if the were anyway. This assumption greatly reduces the complexity of the problem.

### 2.1.3 Impedance models

The ground effect in sound propagation is determined by the impedance of the ground and by the geometrical situation. The ground behavior is strongly dependent on frequency. If we make a few assumptions of the physical properties of the ground, we can construct a theoretical model of the acoustical behavior in the form of an impedance model. We can also construct an empirical model from measured data. The purpose of an impedance model is to describe how the impedance varies with frequency, and possibly how it depends on other physical parameters, such as flow resistivity or porosity. In this text we present one model, which has been used for the calculations in the examples further ahead.

In the examples of this text a model by Delany and Bazley is used. This model is described in [13] and [16], and uses σ, the effective flow resistivity, as a parameter.

$$Z = 1 + 9{,}08\left(\frac{1000f}{\sigma}\right)^{-0{,}75} + i11{,}9\left(\frac{1000f}{\sigma}\right)^{-0{,}73} \qquad (2.2)$$

σ should be around 150 000 - 300 000 for grass, and >20 000 000 for old asphalt, se table 2.1. In figure 2.2 the impedance for σ = 200 000 is plotted. Note that the model predicts high impedance for low frequencies and low impedance for high frequencies. The imaginary part of the impedance is positive, which means that the impedance has a spring-like behavior.

**Table 2.1** Flow resistivities of various ground surfaces, from [12].

| **Description of surface** | **Flow resistivity, in krayls** |
|---|---|
| 1. Dry snow, new fallen 10 cm deep | 15-30 |
| 2. Sugar snow | 25-30 |
| 3. Wood land floor | 50 |
| 4. Grass: rough pasture, airport, public buildings | 150-300 |
| 5. Roadside dirt, ill defined, small rocks up to 10 cm diameter | 300-800 |
| 6. Sandy silt, hard packed by vehicles | 800-2 500 |
| 7. "Clean" limestone chips,thick layer(12,7 to 25,4 mm mesh) | 1 500-4 000 |
| 8. Old dirt roadway, fine stones(6,35 mm mesh), interstices filled | 2 000-4 000 |
| 9. Earth, exposed and rain-packed | 4 000-8 000 |
| 10. Quarry dust, fine, very hard-packed by vehicles | 5 000-20 000 |
| 11. Asphalt sealed by dust and use | > 20 000 |

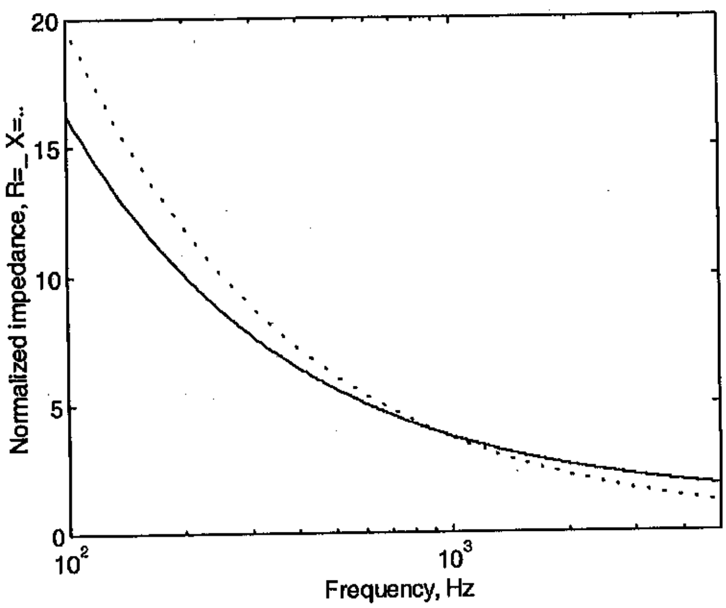


*Figure 2.2*
*Impedance according to [13], σ=200 000*
*— R*
*- - - X*

*Z=R+iX*

### 2.1.4 Plane wave reflection coefficient

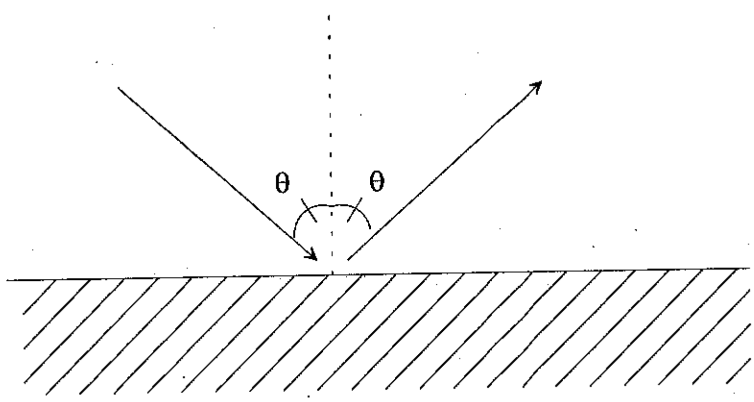


*Figure 2.3*
*Geometry for the plane wave reflection.*

Assume that we have a plane wave propagating towards an infinite plane with normalized impedance Z and admittance $\nu=1/Z$. We also assume that the surface is locally reacting. The angle of incidence is θ. Then we will get a reflected plane wave propagating in a direction given by Snell's law, which in this case is the same angle against the surface normal in figure 2.3. The resulting reflection coefficient is then:

$$R(\theta) = \frac{\cos(\theta) - \nu}{\cos(\theta) + \nu} \tag{2.3}$$

### 2.1.5 Spherical wave reflection coefficient

If we have spherical waves, which we always have if the source is not very far from the surface, we have to calculate a spherical wave reflection coefficient. We use the same assumptions about the surface as in 2.1.4.

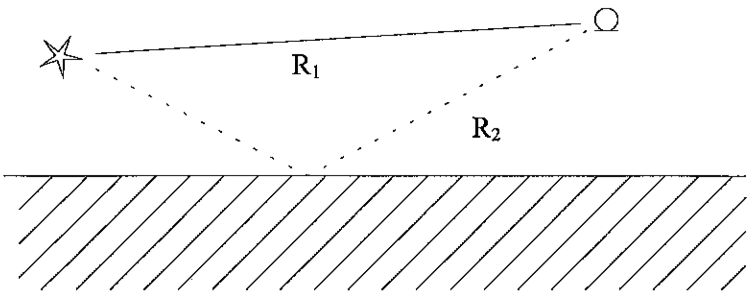


*Figure 2.4 Geometry for the spherical wave reflection.*

This problem was first studied in electromagnetic field theory, and the first paper to solve the problem from the acoustic point of view was by Ingard [15]. After some initial errors from the original article were corrected and other authors have added a few things, the theory can be summarized as follows:

The pressure at a receiver point above a boundary with impedance Z can be expressed as two spherical waves, or rays. One is the direct one and the other one is reflected at the boundary, see figure 2.4.

$$p = \left( \frac{e^{ikR_1}}{R_1} + Q\frac{e^{ikR_2}}{R_2} \right) e^{-i\omega t} \qquad (2.4)$$

The reflected ray is multiplied by the (complex) reflection coefficient Q, which can be calculated by formula (2.5), where R is the plane wave reflection coefficient from formula (2.3).

$$Q = R(\theta) + [1 - R(\theta)]E(\rho) \qquad (2.5)$$

The function E(ρ) is calculated from (2.6), where erfc(z) is the complementary error function extended for complex arguments. ρ is the so called numerical distance calculated from (2.7).

$$E(\rho) = 1 + i\sqrt{\pi}\rho e^{-\rho^2} erfc(-i\rho) \qquad (2.6)$$

$$\rho = \frac{1+i}{2}\sqrt{kR_2}\,(v + \cos(\theta)) \qquad (2.7)$$

One difficulty is to calculate the expression (2.6), but a good solution is to use a series expansion given in [14]. Other functions behave well numerically for most normal source and receiver positions.

In the plane wave case the solution can be seen as an image source multiplied by the reflection coefficient, but in the spherical case it is not as simple. In [1] it is suggested that the spherical reflection can be looked upon as an image source distribution centered on the point given by Snell's law. This can be seen as an infinite number of image sources of infinitesimal magnitude.

The spherical reflection coefficient is almost equal to the plane wave one for high frequencies, which can bee seen in figure 2.5. Note that in the region of 500 Hz there is a minimum, and here the level difference is quite large between Q and R, but the frequency location of the minimum is almost identical.

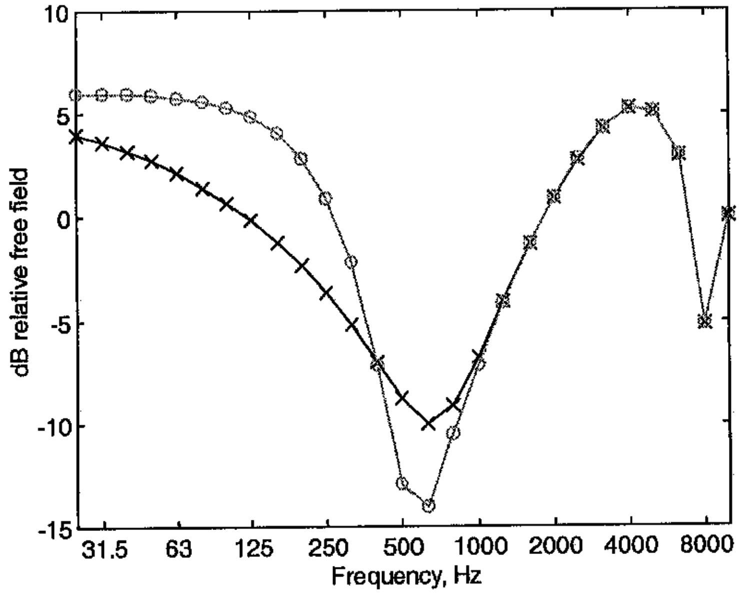


*Figure 2.5*
*Difference between spherical and plane wave reflection coefficient*
*o o spherical (Q=Q)*
*x x plane (Q=R)*
*hs=hr=1 m*
*d=50 m*
*σ=200 000, corresponding to a grass surface.*

### 2.1.6 Pressure relative free field

It is often desirable to study the effect of the ground alone, separate from the effects of geometrical spreading. The usual way to do this is to study the pressure at a point relative to free field. Assume that in a free field case, i.e. without boundary, the pressure at the receiver point is $p_0$, and in the ground case p. Then the pressure relative to free field is $p/p_0$ (2.8). In the spherical wave case the formula for the pressure relative to free field will be, omitting the factor $e^{-i\omega t}$:

$$\frac{p}{p_0} = \frac{\left(\dfrac{e^{ikR_1}}{R_1} + Q\dfrac{e^{ikR_2}}{R_2}\right)}{\dfrac{e^{ikR_1}}{R_1}} = 1 + Q\frac{R_1}{R_2}e^{ik(R_2-R_1)} \qquad (2.8)$$

In the examples of this text all pressures are plotted relative to free field unless otherwise is stated.

## 2.2 Impedance discontinuities

Consider a road with a grass plain next to it. Then the sound source will be above a high impedance surface, the asphalt, and the receiver will be above a lower impedance surface, the grass. How will the change in impedance affect the sound propagation? In the case where the car is very close to the asphalt edge or the receiver is just next to the road, we will in principle have the normal situation with propagation over just one surface. If we are somewhere in between, we have to have another solution though.

### 2.2.1 The de Jong model for impedance discontinuities

A model to deal with impedance discontinuities is described in [8], by de Jong.

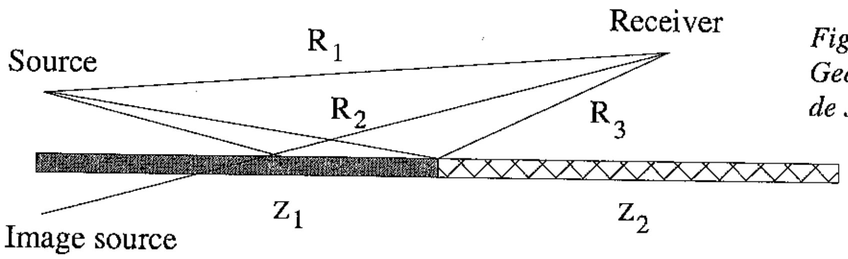


*Figure 2.6 Geometry for the de Jong model.*

If we have the geometry of figure 2.6, the pressure relative to free field can be described by the formulas (2.9) and (2.10), where the former should be used if the point of specular reflection lies on surface 1, and the latter if the point of specular reflection lies on surface 2. If the specular reflection point is exactly the same as the point where the impedance changes, then $R_2$=$R_3$, and the expressions are equal.

$$\frac{p}{p_0} = 1 + \frac{R}{R_2} e^{ik(R_2-R)} Q_1 + (Q_2 - Q_1) \frac{e^{-i\pi/4}}{\sqrt{\pi}} \frac{R}{R_3} \left[ F(\sqrt{k(R_3 - R)}) + F(\sqrt{k(R_3 - R_2)}) e^{ik(R_2-R_1)} \right] \tag{2.9}$$

$$\frac{p}{p_0} = 1 + \frac{R}{R_2} e^{ik(R_2-R)} Q_2 + (Q_2 - Q_1) \frac{e^{-i\pi/4}}{\sqrt{\pi}} \frac{R}{R_3} \left[ F(\sqrt{k(R_3 - R)}) - F(\sqrt{k(R_3 - R_2)}) e^{ik(R_2-R_1)} \right] \tag{2.10}$$

In figure 2.7 we can see the difference for a case where both source and receiver is 1 m above the ground, the distance is 100 m, and the surface changes from asphalt to grass 20 m from the source. Note that even though the point of specular reflection is 30 m from the impedance discontinuity, we still see a strong effect around the point of maximum attenuation.

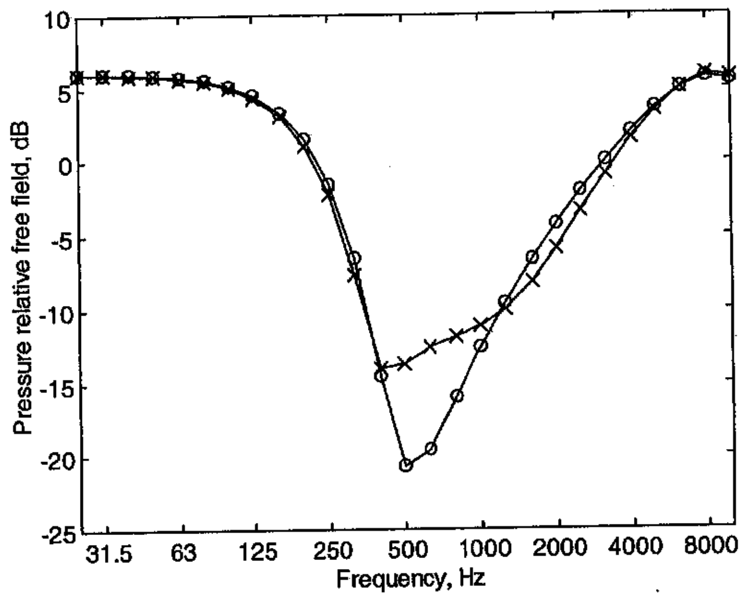


*Figure 2.7*
*de Jong compared to ignoring the hard surface.*
*o o Only grass*
*x x de Jong*
*hs=hr=1 m*
*d=100 m*

*$\sigma_1$=20e6, $\sigma_2$=200 000 corresponding to an asphalt and a grass surface. Asphalt close to source. Discont. 20 m from source.*

The de Jong model has some major drawbacks though. It does not obey the reciprocity condition, which tells us that if we interchange the location of the source and receiver, we get the same result. Furthermore it seems to work only for a hard/soft surface combination, not a soft/hard one. In figure 2.9 some different ways to calculate the resulting pressure from the geometry in figure 2.8 is displayed. PROPAG is a program which uses a numerical method developed by Karsten Bo Rasmussen [9].

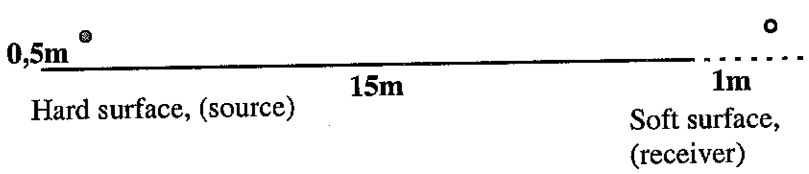


*Figure 2.8*
*Geometry for calculation in figure 2.9*
*$\sigma_1$=20e6, $\sigma_2$=200 000 corresponding to an asphalt and a grass surface.*

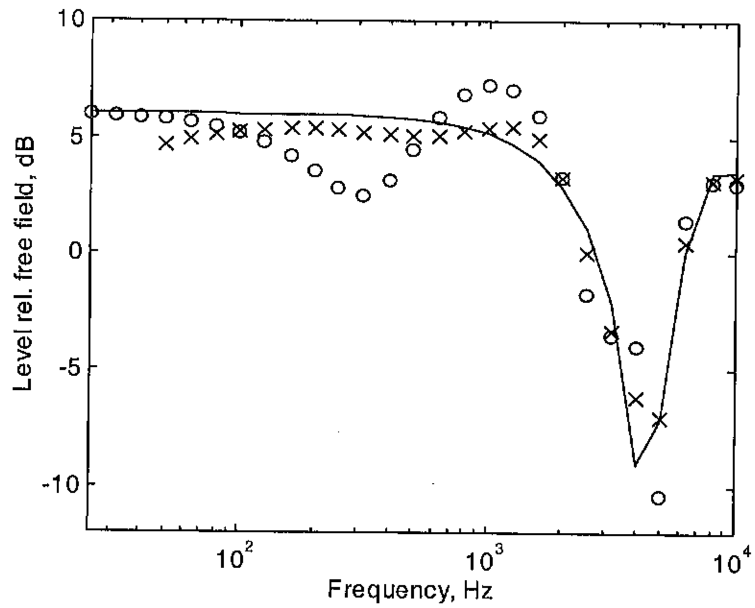


*Figure 2.9*
*de Jong compared to ignoring the soft surface, and to PROPAG from Delta. Geometry as in figure 2.8*

*o o de Jong*
*x x PROPAG*
*— Ignoring the soft side.*

Note that the de Jong solution gives suspicious results in this case (figure 2.9).

## 2.2.2 The Fresnel-zone model

This model [10] is a rather straightforward method. It has been improved by Birger Plovsing to work better in the high frequency region [11]. The model will not be discussed in detail here, but in principle it uses (2.11), where $p_S$ is the solution with the source impedance over the whole surface, $p_R$ the same with the receiver impedance and $p_{TOT}$ is the solution above the plane with the impedance discontinuity. Note that only the absolute value of the solution can be obtained with this method. The weighting factor r is determined by how much of the source side impedance is inside the Fresnel zone, which is an ellipse.

$$20\log(|\, p_{TOT}\,|) = r20\log(|\, p_S\,|) + (1-r)20\log(|\, p_R\,|) \qquad (2.11)$$

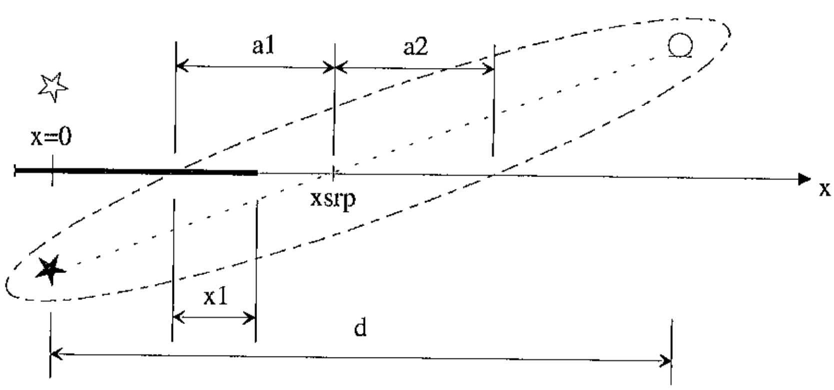


*Figure 2.10*
*Definition of symbols for the Fresnel zone model.*

In the basic model, r is simply the ratio of $x_1$ (if it is >0 ) and the total length of the Fresnel zone, see figure 2.10. If $x_1$ is less than zero, r=0 and the propagation will depend only on the receiver side impedance, and if $x_1$ is greater than $a_1+a_2$ then r=1 and only the source side impedance will affect the propagation.

$$r = \begin{cases} \dfrac{x_1}{a_1 + a_2} & 0 < x_1 \le a_1 + a_2 \\ 1 & x_1 > a_1 + a_2 \\ 0 & x_1 \le 0 \end{cases} \tag{2.12}$$

The Fresnel zone is determined by making an ellipse around the image source and the receiver, and if we use a few approximations we arrive at the expressions (2.13) and (2.14). d is the horizontal distance between source and receiver. C is a portion of the wavelength used to determine the ellipse, and in [10] C=1/4 is recommended.

$$a_1 = \frac{d}{2} \frac{\dfrac{h_S - h_R}{h_S + h_R} + \sqrt{1 + \dfrac{2h_S h_R}{C\lambda d}}}{1 + \dfrac{(h_S + h_R)^2}{2C\lambda d}} \tag{2.13}$$

$$a_2 = \frac{d}{2} \frac{\dfrac{h_R - h_S}{h_S + h_R} + \sqrt{1 + \dfrac{2h_S h_R}{C\lambda d}}}{1 + \dfrac{(h_S + h_R)^2}{2C\lambda d}} \tag{2.14}$$

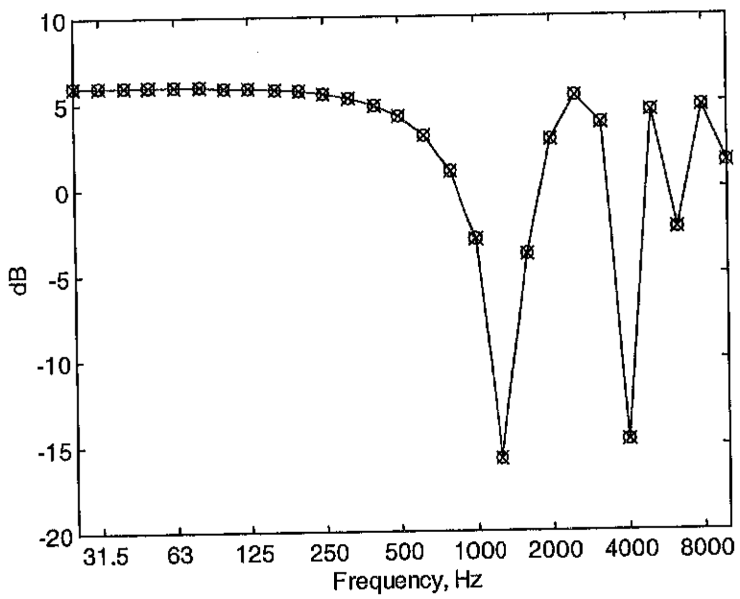


*Figure 2.11 Fresnel-zone calculations compared to neglecting the soft surface. Geometry as in figure 2.8*

*o o Fresnel-zone*
*x x Ignoring the soft side.*

In figure 2.11, the Fresnel-zone model is compared to ignoring the soft surface in the geometry from figure 2.8. As can be expected, there is no difference between the two.

# 3 Diffraction from the semi infinite plane

Under many conditions, a sound barrier can be characterized as a thin screen. This means that the diffracting edge is small in comparison with the wavelength. The simplest solution, without being simple, is for a semi infinite plane. This is a special case of a semi infinite wedge. The exact solution to the wave equation is known in this case for some different boundary conditions, but the calculations are elaborate and it is not possible to implement it using elementary functions.

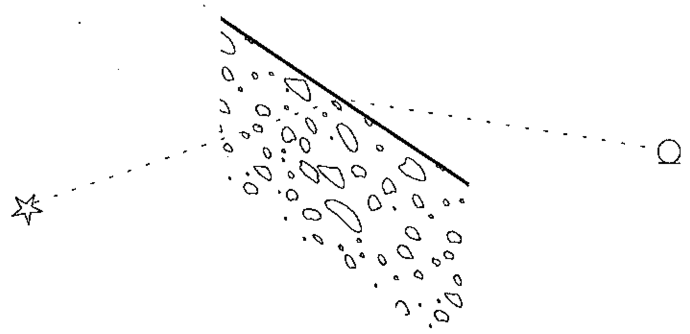

*Figure 3.1*
*The semi infinite plane*

Usually when one talks about diffraction one divides the solution into two parts, the geometrical acoustics part, and the diffracted part. The total solution is the sum of these two parts. In figure 3.2 the semi infinite plane situation is shown divided into three sectors, A,B and C. If we assume that the source is sending out a short pulse, then we will receive different things in the different sectors. In A the direct sound path is cut off by the screen, and the only thing we will receive is a pulse diffracted at the screen top. In B we will also receive a diffracted pulse (even if the receiver is on the same side of the screen as the source), but we will also receive a direct pulse. In sector C we will, in addition to the direct and diffracted pulses, receive a reflected pulse (from the image source).

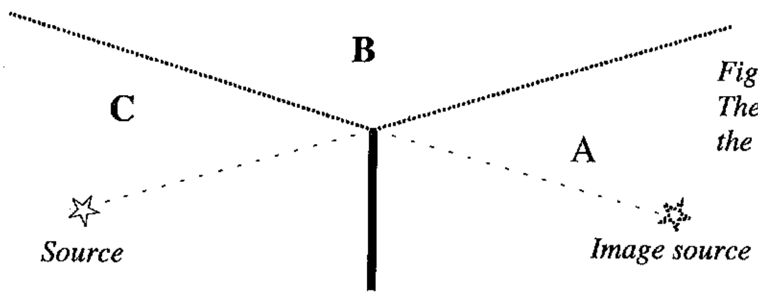


*Figure 3.2*
*The different sectors for the diffracted sound field*

This has the effect that if we only consider the diffracted wave, it will be discontinuous at the boundaries between the sectors.

## 3.1 The Fresnel integral

The so-called Fresnel integral (3.1) and other related functions are very important in the theory of semi infinite plane diffraction.

$$F(x) = \int_x^\infty e^{jt^2}\, dt \tag{3.1}$$

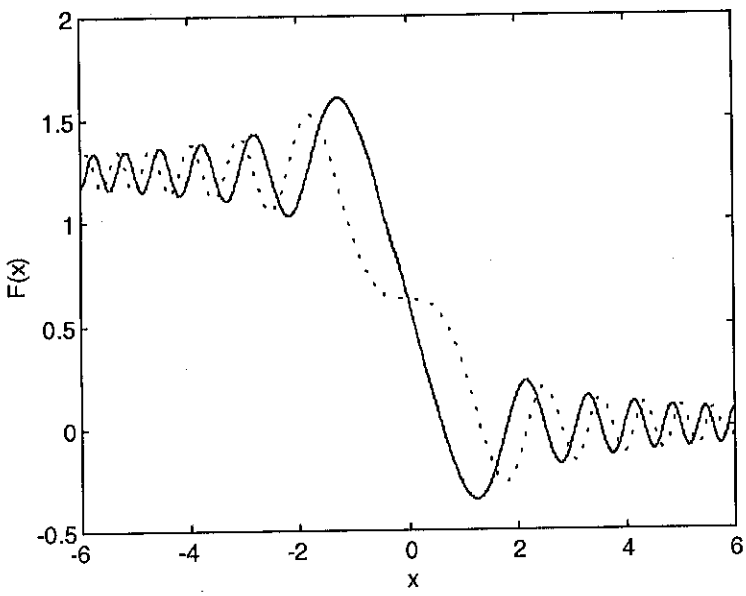


*Figure 3.3*
*Real (—) and imaginary (- - -) parts of the Fresnel integral for x between -6 and 6.*

Note that:

$$F(-x) = \sqrt{\frac{\pi}{2}}(1+i) - F(x) \tag{3.2}$$

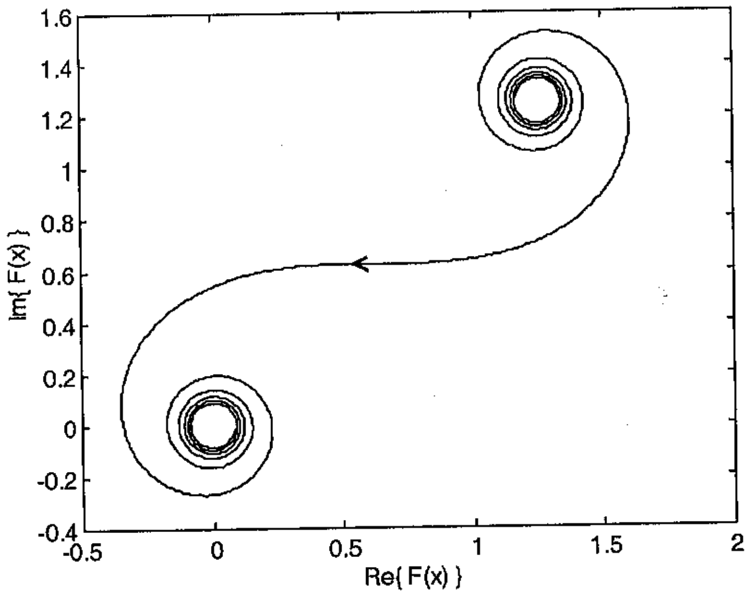


*Figure 3.4*
*Alternative plot for the Fresnel function F(x). The arrow is in the positive x direction. (-6<x<6) (The Cornus spiral)*

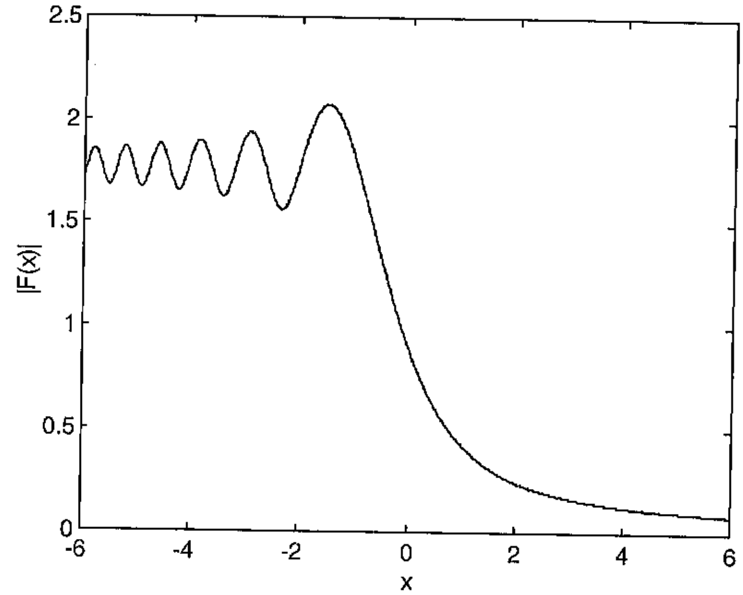


*Figure 3.5*
*Absolute value of the Fresnel integral for x between -6 and 6.*

This function can be expressed in the two functions S(x) and C(x) (3.3).

$$F(x)=\sqrt{\frac{\pi}{2}}\left\{\frac{1}{2}-C(\sqrt{\frac{2}{\pi}}x)+i\left[\frac{1}{2}-S(\sqrt{\frac{2}{\pi}}x)\right]\right\} \qquad (3.3)$$

$$C(x)=\int_0^x \cos(\frac{\pi}{2}t^2)dt$$
$$S(x)=\int_0^x \sin(\frac{\pi}{2}t^2)dt \qquad (3.4)$$

And from C(x) and S(x) we can define the two auxiliary Fresnel functions f(x) and g(x) (3.5).

$$f(x)=\left(\frac{1}{2}-S(x)\right)\cos(\frac{\pi}{2}x^2)-\left(\frac{1}{2}-C(x)\right)\sin(\frac{\pi}{2}x^2)$$
$$g(x)=\left(\frac{1}{2}-C(x)\right)\cos(\frac{\pi}{2}x^2)+\left(\frac{1}{2}-S(x)\right)\sin(\frac{\pi}{2}x^2) \qquad (3.5)$$

As can be seen in figure 3.6, f and g are functions that have asymptotic expressions for large x. These functions are therefore well suited for the calculation of the Fresnel function. The asymptotic expressions are (3.6) (from [4]).

$$f(x)=\frac{1}{\pi x}-\frac{3}{\pi^3x^5}+O(x^{-9})$$
$$g(x)=\frac{1}{\pi^2x^3}-\frac{15}{\pi^4x^7}+O(x^{-11}) \qquad (3.6)$$

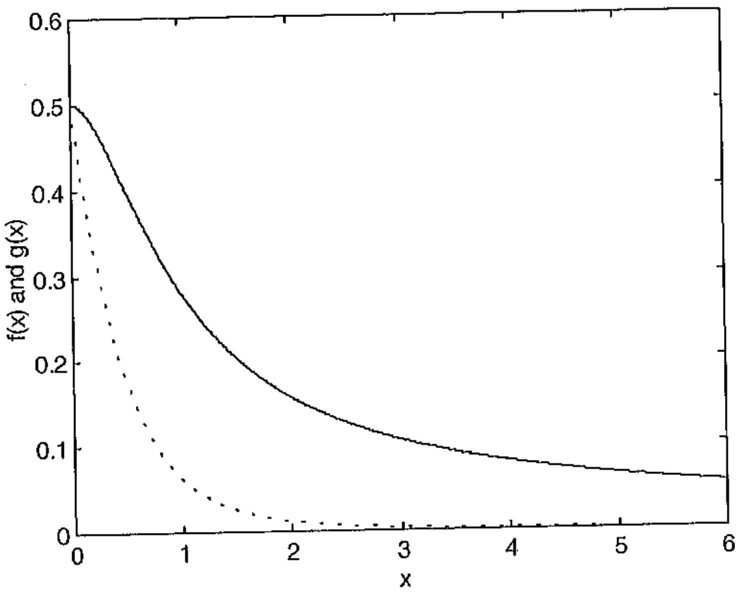


*Figure 3.6*
*The auxiliary Fresnel functions f(x) ( —) and g(x) ( - - - ).*

The question is how to handle small values for x. One possibility is to assume a polynomial and to fit it to numerical calculations of f and g for small x. A polynomial fit for 0<x<5 is presented in table 3.1.

$$f(x) = a_0 + a_1 x + a_2 x^2 + \ldots \tag{3.7}$$

| 0<x<5 | f(x) | g(x) |
|---|---|---|
| $a_{12}$ | 0.00000019048125 | -0.00000151974284 |
| $a_{11}$ | -0.00000418231569 | 0.00005018358067 |
| $a_{10}$ | 0.00002262763737 | -0.00073624261723 |
| $a_9$ | 0.00023357512010 | 0.00631958394266 |
| $a_8$ | -0.00447236493671 | -0.03513592318103 |
| $a_7$ | 0.03357197760359 | 0.13198388204736 |
| $a_6$ | -0.15130803310630 | -0.33675804584105 |
| $a_5$ | 0.44933436012454 | 0.55984929401694 |
| $a_4$ | -0.89550049255859 | -0.50298686904881 |
| $a_3$ | 1.15348730691625 | -0.06004025873978 |
| $a_2$ | -0.80731059547652 | 0.80070190014386 |
| $a_1$ | 0.00185249867385 | -1.00151717179967 |
| $a_0$ | 0.49997531354311 | 0.50002414586702 |

*Table 3.1*
*Polynomial expression (least-squares approximation) of the auxiliary Fresnel functions f and g for small x. 0<x<5*

## 3.2 The Pierce solution

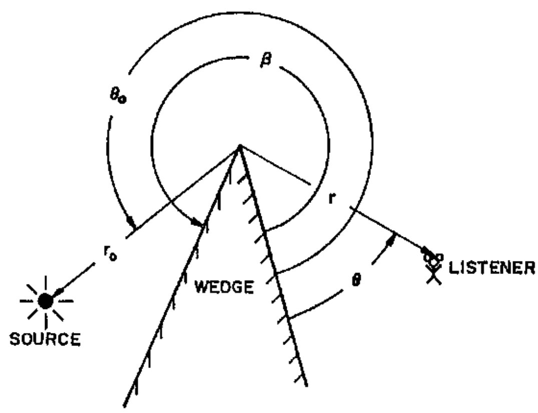


*Figure 3.7 Definition of symbols, from [4].*

In [1] a solution for the semi infinite wedge diffraction is presented. If the wedge angle β is $2\pi$ then this corresponds to the semi infinite plane case. The solution is based on the function $A_D(x)$, which is defined in (3.8). $A_D(x)$ is best calculated from the auxiliary Fresnel-functions f(x) and g(x) (3.6).

$$A_D(x) = \frac{\sqrt{2}}{2\pi} \int_{-\infty}^{\infty} \frac{e^{-u^2}}{(\pi/2)^{1/2} x - e^{-i\pi/4} u} du = sign(x)\left[f|x| - ig|x|\right] \qquad (3.8)$$

The solution $p_{Diffr}$ (3.9) is defined for all r, θ and z, where r and θ is defined in figure 3.7, and z is defined as in standard cylindrical coordinates. The distance between the source and the receiver is L.

$$p_{Diffr}(r,\theta,z) = \frac{e^{ikL}}{L} \frac{e^{i\pi/4}}{\sqrt{2}} \left(A_D(X_+) + A_D(X_-)\right) \qquad (3.9)$$

where

$$X_+ = X(\theta + \theta_0) \qquad X_- = X(\theta - \theta_0) \qquad (3.10)$$

$$X(\theta) = \sqrt{\frac{2r_0 r}{\lambda L}} \frac{\cos(\nu\pi) - \cos(\nu\theta)}{\nu \sin(\nu\pi)} \qquad (3.11)$$

If we study only $p_{Diffr}$, we will notice that it is discontinuous around the line of sight (LOS, the border between zone A and B, see figure 3.2. This can be seen in figure 3.9 and 3.10, where the absolute value of $p_{Diffr}$ is displayed in a contour plot.

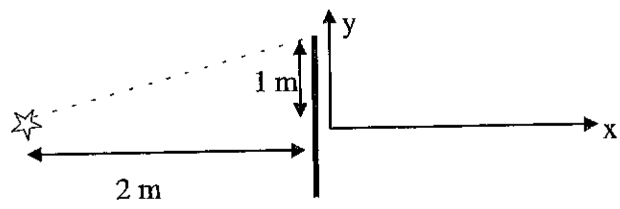


*Figure 3.8*
*Source position and definition of axes x and y for figures 3.9 and 3.10*

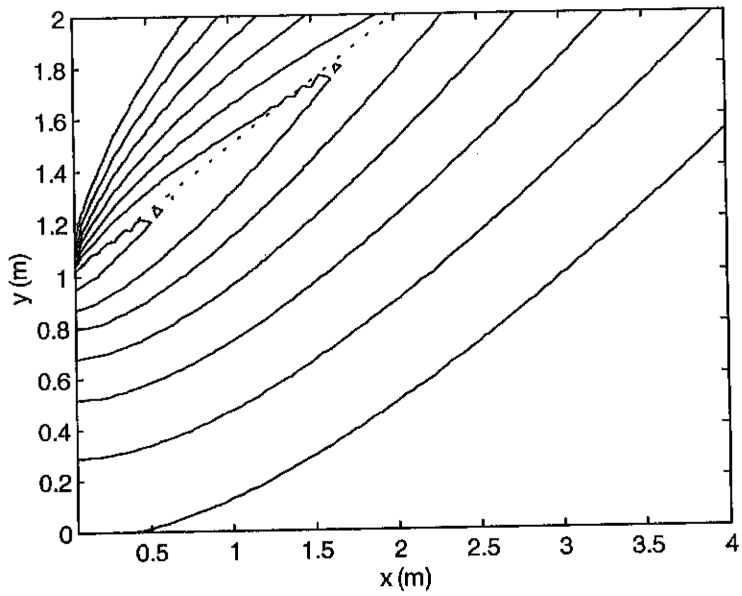


*Figure 3.9*
*Contour plot of the diffracted field only ($p_{Diffr}$). see figure 3.8. The dotted line represents the line of sight. Note that the field is discontinuous around the LOS.*

*f=1000 Hz*

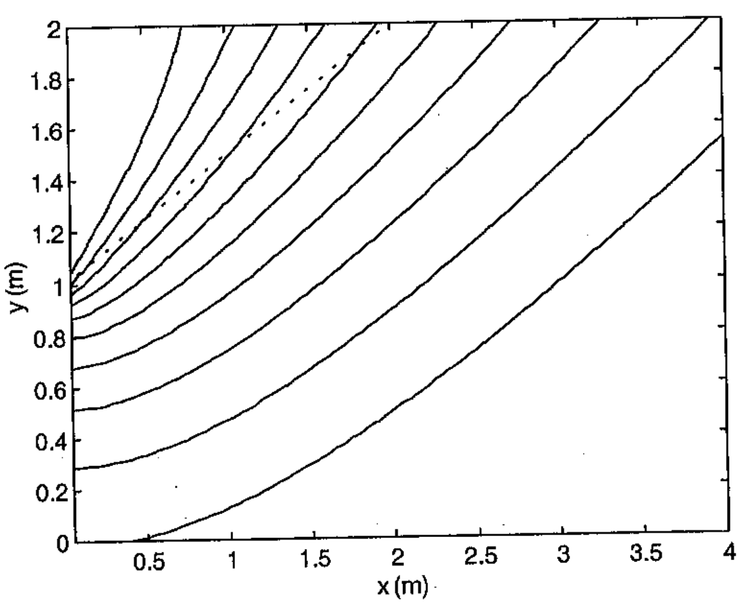


*Figure 3.10*
*Contour plot of the diffracted field and a direct part added above the line of sight. ($p_{Diffr}$+$p_{Direct}$). See figure 3.8. The dotted line represents the line of sight. Note that the sum is continuous.*

*f=1000 Hz*

## 3.3 The Macdonald solution

In [6] H. Jonasson presents a way to calculate the semi infinite diffraction for a hard or pressure release screen. Pressure release corresponds to a reflection factor of -1 for all frequencies, and a model for an absorbing screen can be obtained by taking away the second term. The solution is based on an exact solution by Macdonald [7]. The diffracted field is given by (3.12)

$$p_d = \frac{e^{i\pi/4}}{\sqrt{\pi}}\left\{\frac{e^{ikR}}{kR_x}F(x) \pm \frac{e^{ikS}}{kS_y}F(y)\right\} \qquad (3.12)$$

The sign ± is + for a hard screen, and - for a pressure release screen, and the second term is removed to simulate an absorbing screen. Note however that this solution uses the free field wave (3.13), so we have to divide by this expression to get a solution relative to free field conditions.

$$p_0 = \frac{e^{ikR}}{kR} \qquad (3.13)$$

The parameters $R_x$ and $S_y$ are defined in (3.14).

$$R_x = \sqrt{\frac{(R_1 + R)R_1}{2}}$$
$$S_y = \sqrt{\frac{(R_1 + S)R_1}{2}} \qquad (3.14)$$

R is the distance between the source and the receiver, and S is the distance between the image source and the receiver. $R_1$ is the shortest way over the screen from the source to the receiver.

$$x = -\sqrt{\frac{krr_0}{R + R_l}}\cos(\theta - \theta_0)$$
$$y = -\sqrt{\frac{krr_0}{S + R_l}}\cos(\theta + \theta_0) \qquad (3.15)$$

$r_0$, $r$, $\theta_0$ and $\theta$ is defined in figure 3.7. Note that $\beta = 2\pi$ in this case.

## 3.4 The Hadden/Pierce solution

In [5] a solution by Hadden and Pierce is presented, and since it is a four rays model, we can apply a spherical reflection coefficient to the image rays and thus get a solution for a wedge or screen with any impedance on its surface. The main equation is (3.16), which is a sum of four terms.

$$p_{Diffr} = -\frac{1}{\pi}\sum_{n=1}^{4} A(\Phi_n)E_v(A(\Phi_n))\frac{e^{ikR}}{R} \tag{3.16}$$

The function $E_v$ is defined in (3.17). Note that here is $\nu$ the wedge index, and not the admittance. The wedge index is $\nu=\pi/\beta$.

$$E_v = \frac{\pi}{\sqrt{2}}\frac{\sin|A|}{|A|}\frac{e^{i\pi/4}}{\sqrt{1+\left(\frac{2r_S r_R}{R^2}+\frac{1}{2}\right)\frac{\cos^2|A|}{\nu^2}}}A_D(B) \tag{3.17}$$

$A_D$ is the function defined in (3.8), and B is given by (3.18).

$$B = \sqrt{\frac{4kr_S r_R}{\pi R}}\frac{\cos|A|}{\sqrt{\nu^2+\left(\frac{2r_S r_R}{R^2}+\frac{1}{2}\right)\cos^2|A|}} \tag{3.18}$$

A is given in (3.19). H is the step function (3.20).

$$A \equiv A(\Phi_n) = \frac{\nu}{2}(-\beta-\pi+\Phi_n)+\pi H(\pi-\Phi_n) \tag{3.19}$$

$$H(x) = \begin{cases} 1 & x \geq 0 \\ 0 & x < 0 \end{cases} \tag{3.20}$$

The four different arguments $\Phi_n$ corresponds to the four rays in the wedge case (3.21).

$$\begin{aligned} \Phi_1 &= |\theta_R - \theta_S| \\ \Phi_2 &= \theta_R + \theta_S \\ \Phi_3 &= 2\beta - (\theta_R + \theta_S) \\ \Phi_4 &= 2\beta - |\theta_R - \theta_S| \end{aligned} \tag{3.21}$$

If we want to calculate the same thing for a wedge with impedance $Z_S$ on the source side and $Z_R$ on the receiver side, we multiply the "rays" with the corresponding spherical reflection coefficient $Q_S$ and $Q_R$. In formula (3.16) for $p_{Diffr}$ we multiply the second term with $Q_S$, the third with $Q_R$ and the forth with $Q_SQ_R$. $Q_S$ is calculated with $r_S$ as the distance parameter and the reflection angle is the angle against the impedance plane ($Z_S$). $Q_R$ is calculated in the same way but with $r_R$ and the angle against the impedance plane ($Z_R$) as parameters.

This model is, with my implementation, about 90 % slower (in terms of floating point operations per second) than 3.2. If we use the method presented above to calculate the diffraction with impedance on the screen sides, the calculation will be much slower because we have to calculate the spherical reflection coefficients.

# 4 Combining diffraction and ground effect

A noise barrier is often placed on the ground. As we have seen, a barrier can be considered as a semi infinite plane in terms of diffraction, and the ground can be handled by the spherical reflection coefficient. Now we have to combine these two effects into a single model for the sound propagation around screens on the ground. If we use a numerical approach such as boundary element methods or the method presented in [2], then we will have the total solution. If we use the analytical models presented here, we must find a method to combine them into a "heuristic" solution.

## 4.1 The image method

The method described by Hans Jonasson in [6] uses an image source and an image receiver to form four rays, or possibly more if direct rays are not screened, together with the semi infinite plane diffraction to form the pressure on the receiver side of the screen. This method is valid if the diffraction from the corners between the ground and screen sides can be neglected. Note that if the ground and the screen have the same impedance, there is no diffraction from the corners. Normally there is, and it can only be neglected if the height of the screen is large in comparison to the wavelength.

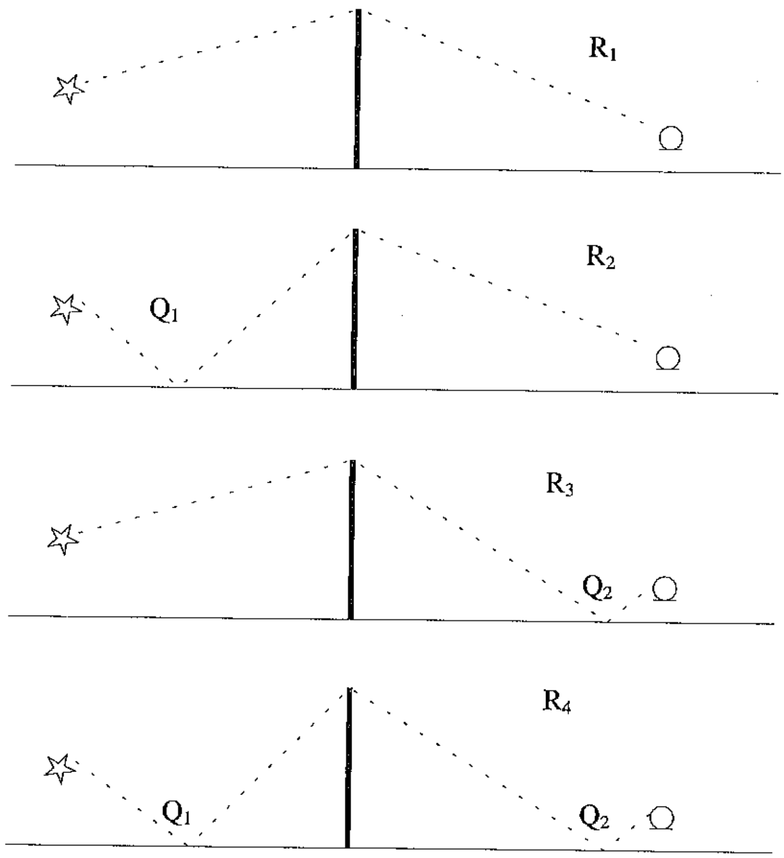


*Figure 4.1*
*Figure of the four rays in the image method of combining ground effect and diffraction over a thin screen.*

$$p = p_1 + p_2Q_1 + p_3Q_2 + p_4Q_1Q_2 \tag{4.1}$$

In formula (4.1), $p_n$ is the pressure from the (image) source to the (image) receiver over a semi infinite plane. The spherical reflection coefficient $Q_1$ and $Q_2$ are calculated as if the source ($Q_2$) or the receiver ($Q_1$) is located at the screen top.

## 4.2 Model measurement of a thin screen

To verify the thin screen model, a series of model measurements were made in the hemi-anechoic chamber at SP. A screen was constructed of 13-mm gypsum boards, and placed on the concrete floor, se figure 4.2. The source consists of four nozzles blowing pressurized air against a common point located about 2 mm above the concrete floor.

*Figure 4.2*
*Model measurements of a thin screen. The screen width is 13mm, which corresponds to a "wide" frequency limit of about 26 kHz*

In figure 4.3 we can a comparison between the measurements and a theoretical value calculated with the Hadden/Pierce diffraction model. The floor and the screen is assumed to be rigid (Q=1), and the source and receiver heights is set to zero. The systematical error in the measured values probably comes from a drift in the static source pressure between reference and screen measurements, since for this measurement the source was turned off between the two. For the other model measurements described later, the source was kept running to ensure the same source level.

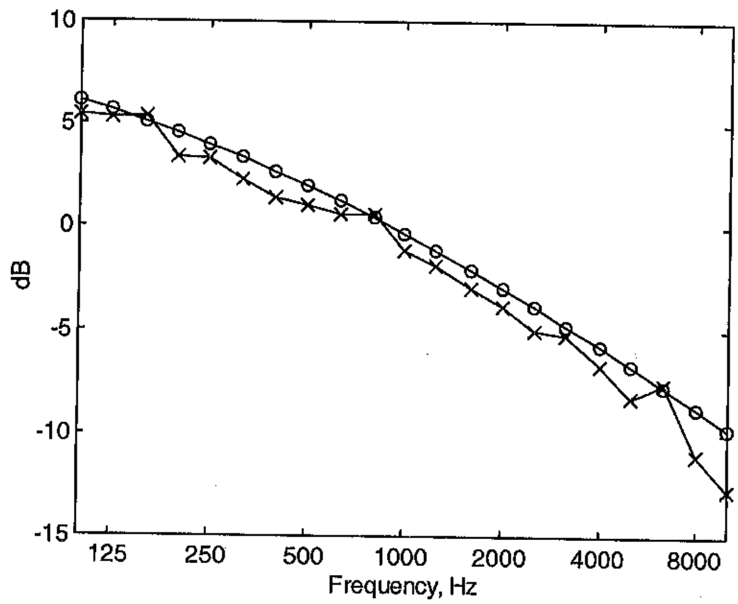


*Figure 4.3*
*Model measurements and theoretical calculations using the Hadden/Pierce diffraction model for a thin screen case.*

*x x Measurement*
*o o Theory*

*hs=hr=0, d=170 cm, ds=100 cm, hsc=30 cm*

## 4.3 Low screens

When the screen height goes to zero, the solution should approach that for a point source above an impedance plane. The model in 4.1 does not, which can easily be seen in (4.1).

If we have a screen which is 1cm high, and our wavelength is 1m, then the screen should not affect the propagation at all. One way to achieve this would be to calculate as an ordinary plane ground, or plane ground with impedance jump, and just ignore the screen. If we choose the limiting case to be when the screen height equals one tenth of a wavelength, we get the formula (4.2), where $h_{SC}$ is the screen height, for the frequency where the screen cease to affect the propagation. We can then use the method described in 5.1.3 to merge the solution with the screen and the solution without a screen into one.

$$f = \frac{c}{10h_{sc}} \qquad (4.2)$$

# 5 Multiple diffraction

## 5.1 Wide barriers

When the barrier is wide in comparison to the wavelength, the diffracted wave will be weaker (at least in average) in the shadow region than if only an infinitely thin screen were present.

### 5.1.1 The Pierce solution to wide barriers

In [4] a solution to the double wedge case, see figure 5.1, is presented. It is basically the same as the solution in 3.2.

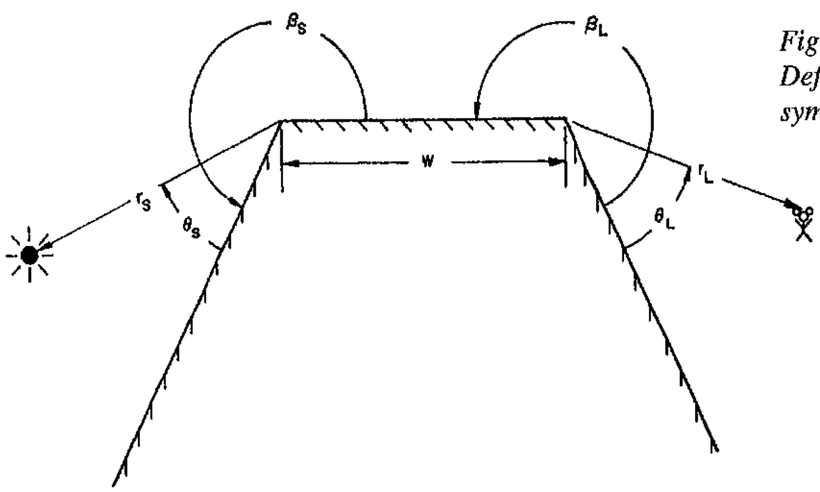


*Figure 5.1 Definition of symbols, from [4].*

The expression for the diffracted field $p_D$ is given in (5.1). Note that this solution is valid only if $\beta_S$-$\theta_S$>$\pi$ and $\beta_L$-$\theta_L$>$\pi$. Another restriction is that kw>>1, which means that the top surface must be larger than one wavelength for the model to be correct.

$$p_D = \frac{ie^{ikL}}{L}\left(f(Y_>) - ig(Y_>)\right)\left(f(BY_<) - ig(BY_<)\right) \qquad (5.1)$$

L is the distance between the source and receiver along the top of the barrier, $r_S$+$r_R$+w if there is no difference in z-coordinate, which is the only case I study. f and g are the so called auxiliary Fresnel functions, see 3.1.

$$\gamma_S = \sqrt{2r_S(w+r_L)/\lambda L} \qquad (5.2)$$

$$Y_S = \gamma_S M_{\nu S}(\beta_S - \theta_S) \qquad (5.3)$$

$Y_<$ is the minimum, and $Y_>$ the maximum of $Y_S$ and $Y_L$, where $Y_S$ (and $Y_L$ with a change of the indices) can be calculated according to (5.2) and (5.3). The function $M_\nu(\Theta)$ is defined in (5.4).

$$M_v(\theta) = \frac{\cos(v\pi) - \cos(v\theta)}{v\sin(v\pi)} \tag{5.4}$$

The main disadvantage with this method is that the surfaces must be hard, and that the top surface must be at least one wavelength long.

### 5.1.2 The Salomons solution to wide barriers

The method described under 5.2 can also be used to calculate a total diffraction coefficient for the wide barrier case. Just set $\beta=3\pi/2$ for the diffracting edges, and M=1. Then we can have any impedance on the surfaces, and we can use any receiver and source positions. We still have to have all surfaces at least a wavelength long to get the correct result though, which means that wide barriers are only wide if they are wide in comparison to the wavelength. The screen width is usually the limiting parameter.

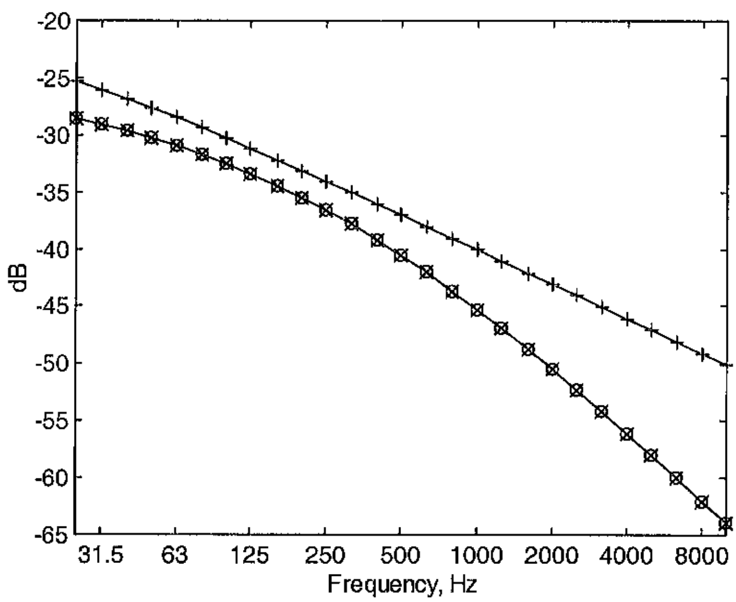


*Figure 5.2 Diffraction from a wide screen.* $\theta_s=\theta_L=\pi/4$, $r_S=r_L=4m$, $w=0.34m$ *Screen surface is hard.*

*x x Pierce*
*o o Salomons*
*+ + Single edge diffraction, w=0.*

In figure 5.2 the wide screen solution of Pierce and Salomons are compared, and they are exactly equal. In this case the screen is 34 cm wide, corresponding to a limiting frequency of 1 kHz. Below this frequency, the solution should be like the single edge diffraction.

### 5.1.3 Frequency condition for wide barriers

Both wide screen models have the condition that the barrier width must be one wavelength or larger. For lower frequencies there exists no solution, but the single edge solution should be very close to the true solution. We should like to be able to mix the two models, and here follows a simple idea how to merge them:

> Calculate the limit frequency f (=c/w) where $w=\lambda$. From the first third octave band where the center frequency is larger than f, choose the double diffraction solution. For the lower third octave bands, add the solutions with a weighting factor r according to $P_{TOT}=(1-r)P_{Double}+rP_{Single}$ where r is 0.2, 0.4,0.6,0.8 and 1 for the remaining third octave bands in descending order.

*Table 5.1*
*Merging of single and double diffraction.*

| Frequency, kHz | 0.315 | 0.4 | 0.5 | 0.63 | 0.8 | 1 | 1.25 | 1.6 |
|---|---|---|---|---|---|---|---|---|
| Single diffraction, dB | -35.1 | -36.1 | -37.1 | -38.1 | -39.1 | -40.1 | -41.1 | -42.1 |
| Multiply with | 1.0 | 1.0 | 0.8 | 0.6 | 0.4 | 0.2 | 0.0 | 0.0 |
| Double diffraction, dB | -37.9 | -39.3 | -40.6 | -42.1 | -43.7 | -45.3 | -46.9 | -48.8 |
| Multiply with | 0.0 | 0.0 | 0.2 | 0.4 | 0.6 | 0.8 | 1.0 | 1.0 |
| Add for total solution | -35.1 | -36.1 | -37.8 | -39.7 | -41.9 | -44.2 | -46.9 | -48.8 |

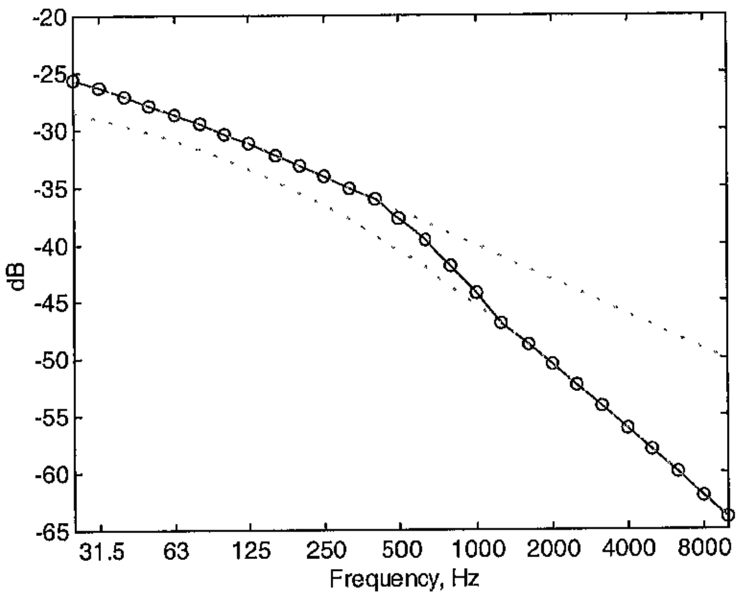


*Figure 5.3*
*Diffraction from a wide screen.*
*$\theta_s=\theta_L=\pi/4$,*
*$r_S=r_L=4m$, $w=0.34m$*
*Screen surface is hard. The solution is obtained by merging the single and double edge solutions.*

*- - Single and double edge solutions*
*o Merged solution*

## 5.1.4 Model measurement of a wide barrier

To test the validity of the wide screen solution a model measurement was carried out in SP's hemi-anechoic room. The source is described briefly in 4.2. A more complete presentation of the measurements can be found in annex A.

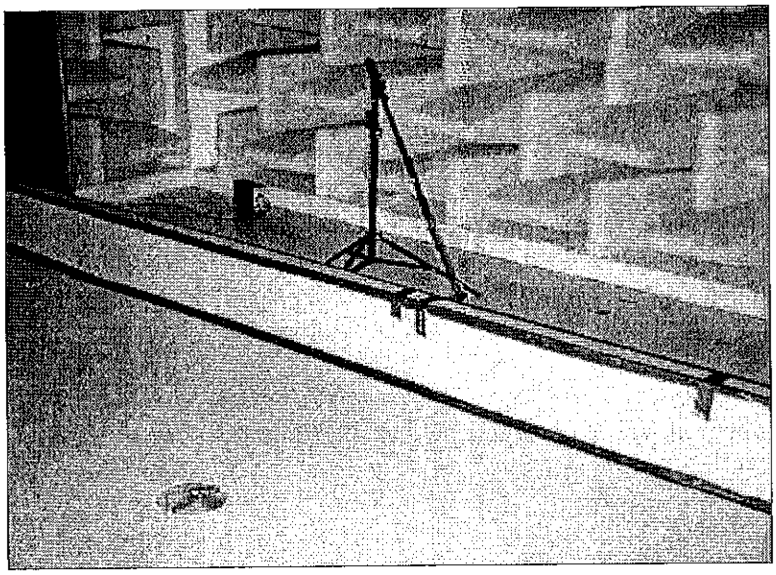

*Figure 5.4*
*Model measurements of a wide screen. The screen width is 10 cm, which corresponds to a wide frequency limit of 3400 Hz*

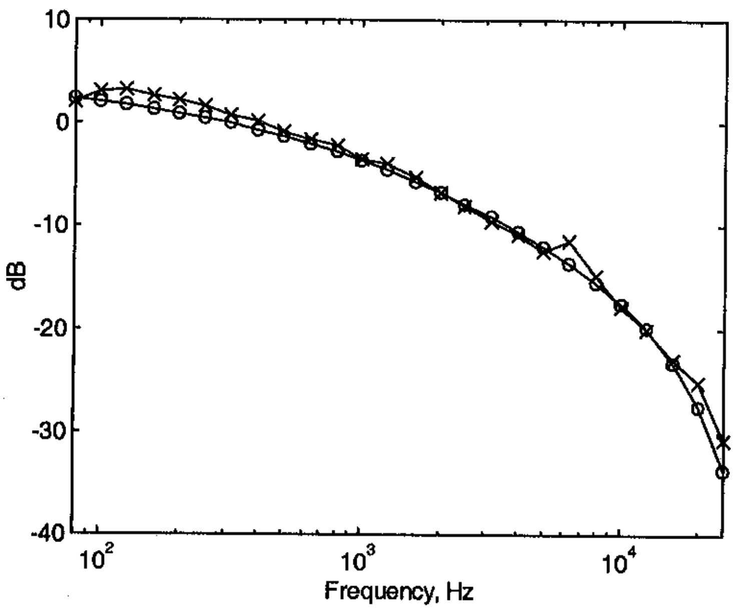


*Figure 5.5*
*Comparison between model measurements and theory for a wide screen. The screen width is 10 cm, which corresponds to a wide frequency limit of 3400 Hz*

*x Measurement*
*o Theory*

In figure 5.5, we can see the pressure relative free field behind a wide screen both for a model measurement and for a calculation using the wide barrier solution by Pierce. The barrier is 10 cm wide, so for frequencies lower than 3400 Hz we should use a single edge solution, which would increase the values somewhat. Due to the source, all measured values below 500 Hz are unreliable. The source is too weak in comparison with the background noise level in this region.

## 5.2 Multiple screens

For a situation with many diffracting edges, such as two screens after each other, the solutions presented earlier can not be applied directly, but in [3] a method to use the simple wedge diffraction to solve multi screen cases is presented. The idea is to calculate the diffraction using equivalent sources, and then combine the diffraction coefficients to a total diffraction with a special scheme. [3] also shows how a diffraction model for a semi infinite wedge can be used to calculate the effects of impedance jumps. Furthermore the text deals with non parallel wedges, and non infinite wedges, but this is not considered here.

If we assume that the diffraction over a wedge can be described as a function $D=D(r_R,r_S,R,\theta_R,\theta_S,\nu,k)$, where D is defined by (5.5), and the diffraction model chosen.

$$p_{Diffr} = D\frac{e^{ikR}}{R} \qquad (5.5)$$

If we limit ourselves to cases where the source and receiver are located on the same z-coordinate, then the distance $R=r_R+r_S$. To find the total combined diffraction coefficient for a given geometry, do as follows (from [3]):

- Start by calculating the diffraction coefficient $D_i$ for each diffracting edge, using the previous edge (or the source) as the source and the following edge (or the receiver) as the receiver. Salomon proposes that this should be done for only one frequency, and he uses 270 Hz. We could also do this for all frequencies for which we calculate, but then we would get small discontinuities in the spectrum.

- Modify the coefficients $D_i$ by choosing $s_{ri}=R_i+R_{i+1}+\ldots+R_{j-1}$ , with $|D_j| < |D_i|$ , and $s_{si}=R_{j+1}+R_{j+2}+\ldots+R_i$ , with $|D_j| < |D_i|$
  $S_i = s_{ri} + s_{si}$
  The new $D_i=D(s_{ri},s_{si},S_i,\theta_{ri},\theta_{si},v_i,k)$ are calculated for all frequencies. In other words, you exchange the source and receiver points to the nearest edge with $|D_j| < |D_i|$
  And the total diffraction coefficient is:
  $$D_{tot} = \left(\frac{1}{2}\right)^{M} D_1 D_2 \ldots D_N \qquad (5.6)$$
  Where M is number of wedges with a common side plane, and N is the number of edges.

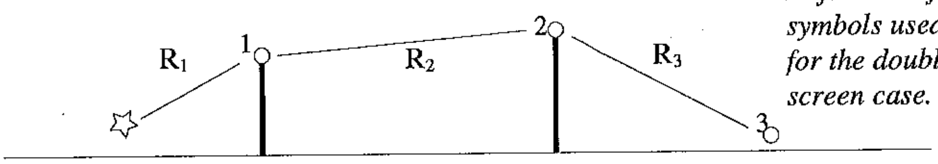


*Figure 5.6 Definition of symbols used above for the double screen case.*

Note that this method is heuristic, and most likely the accuracy of the method decrease as the number of diffracting edges and the number of reflecting planes increase. Furthermore, the number of rays increase as $2^N$, so the method will be slow for complicated problems. On the other hand most of the rays will have a negligible contribution to the overall sound pressure, since a ray diffracted many times will be very weak.

### 5.2.1 The double screen case

The method above is perhaps best described by an example, so we study the double screen above an impedance plane situation, se figure 5.7.

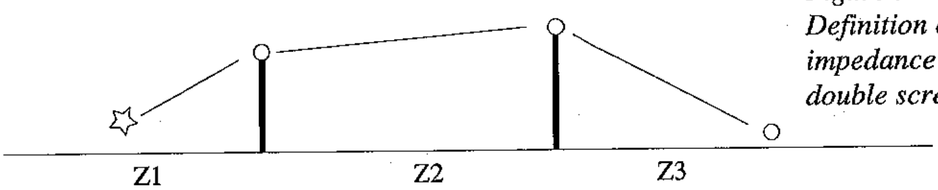


*Figure 5.7 Definition of impedance for the double screen case.*

We can see this as two diffracting edges, and three reflecting planes. In this case we will have 2^(N+1) = 8 rays, and possibly a direct ray also. Each ray can be calculated with the method described above. Then we add the rays multiplied with the spherical reflection coefficients appropriate to the situation.

One way to represent this is to use image screens. In figure 5.8 the first four rays for the two-screen situation is presented, and the last four are in figure 5.9, with the exception of the direct ray if present. Now we use the method described above to calculate the total diffraction coefficient $D_{tot}$ for each ray, and add them according to (5.7).

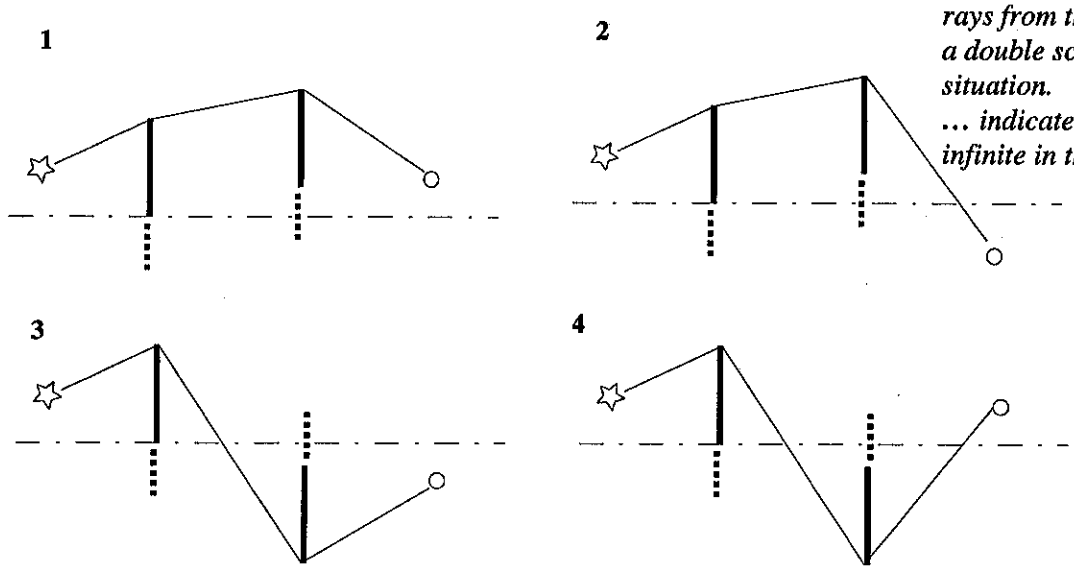


*Figure 5.8*
*Illustration of the four rays from the source in a double screen situation.*
*... indicates screen infinite in this direction*

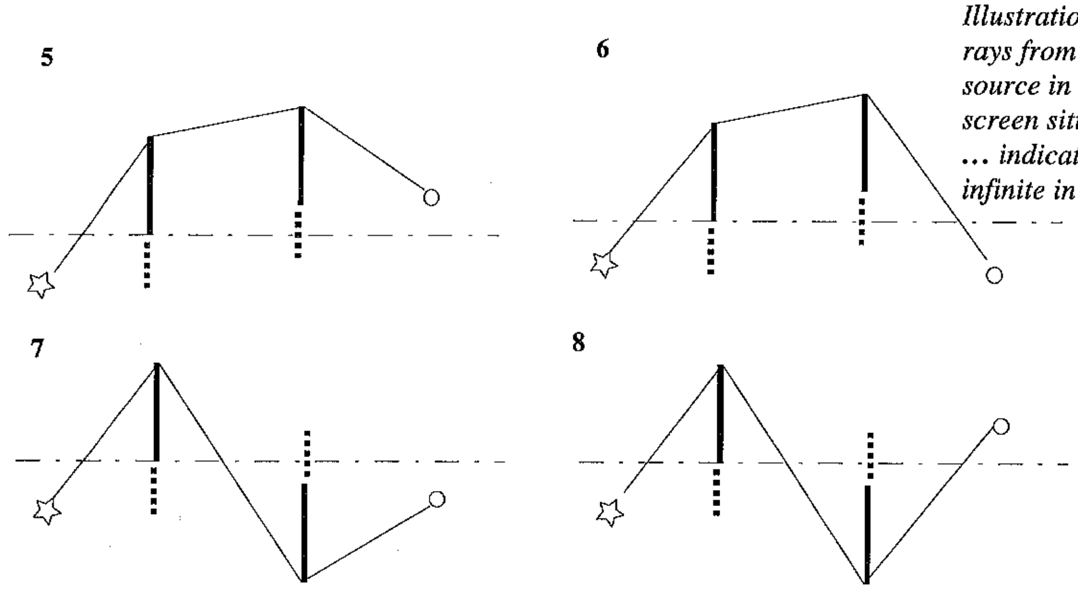


*Figure 5.9*
*Illustration of the four rays from the image source in a double screen situation.*
*... indicates screen infinite in this direction*

$$
\begin{aligned}
p = {} & D_1 \frac{e^{ikR_1}}{R_1} + D_2 \frac{e^{ikR_2}}{R_2} Q_3 + D_3 \frac{e^{ikR_3}}{R_3} Q_2 + D_4 \frac{e^{ikR_4}}{R_4} Q_2 Q_3 + \\
& + D_5 \frac{e^{ikR_5}}{R_5} Q_1 + D_6 \frac{e^{ikR_6}}{R_6} Q_1 Q_3 + D_7 \frac{e^{ikR_7}}{R_7} Q_1 Q_2 + D_8 \frac{e^{ikR_8}}{R_8} Q_1 Q_2 Q_3
\end{aligned}
\tag{5.7}
$$

$Q_1$ is calculated with the normal source and the first screen top as the receiver, $Q_2$ with the first as the source and the second as the receiver, and $Q_2$ with the second as the source and the normal receiver. $R_n$ is the length of ray number n.

### 5.2.2 Model measurement of double screen

To verify the double screen solution, a model measurement was made in the hemi-anechoic room at SP, se figure 5.10. The source is briefly described in 4.2. A more complete presentation of the measurements can be found in annex B.

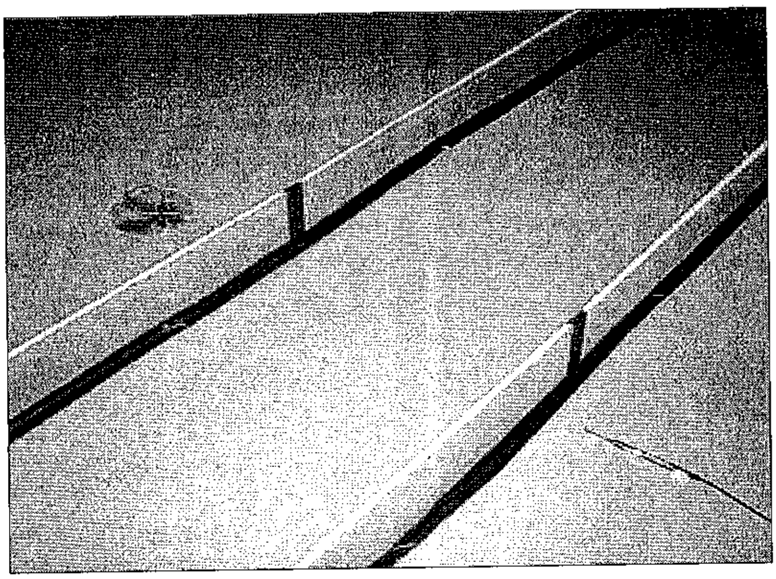

*Figure 5.10*
*Model measurement of a double screen case. The distance between the screens is 70 cm, source to screen one 30 cm, screen two to the source 10 cm. Both source and receiver is at height 0.*

In figure 5.11 we can see a comparison of the model measurement and the theory described above. As before, the source is very weak below 500 Hz, so these values are unreliable in the measured case.

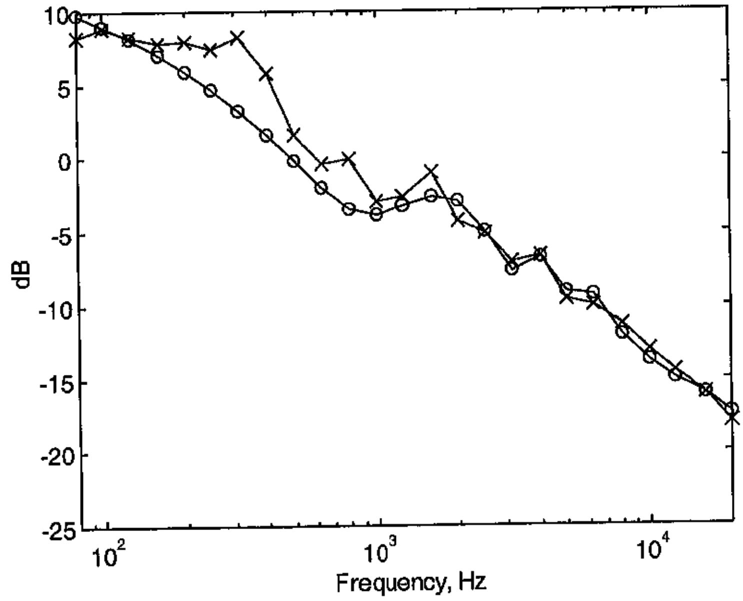


*Figure 5.11*
*Comparison between model measurements and theory for a double screen case. The distance between the screens is 70 cm, source to screen one30 cm, screen two to the receiver 10 cm. Both source and receiver is at height 0.*

*x x Measurement*
*o o Theory*

# 6 References

[1] Tutorial on sound propagation outdoors
Tony F. W. Embleton
J. Acoust. Soc. Am. 100(1) 1996

[2] Diffraction by a screen above an impedance boundary
Sven-Ingvar Thomasson
J. Acoust. Soc. Am. 63(6) 1978

[3] Sound Propagation in Complex Outdoor Situations with a Non-Refracting Atmosphere: Model based on Analytical Solutions for Diffraction and Reflection
Erik M. Salomons
Acustica / acta acustica 83, 1997

[4] Diffraction of sound around corners and over wide barriers
Allan D. Pierce
J. Acoust. Soc. Am. 55(5) 1974

[5] Sound diffraction around screens and wedges for arbitrary point source locations
W. James Hadden, Allan D. Pierce
J. Acoust. Soc. Am. 69(5) 1981

[6] The Propagation of Sound Over Ground With and Without Acoustic Barriers
H. Jonasson
Report 18, Division of Building Technology, Lund (Sweden) 1971

[7] A Class of Diffraction Problems
H. M. Macdonald
Proceedings of the London Mathematical Society, 14, 1915

[8] Rekenmodellen om de invloed te voorspellen van een asfalt-grasovergang en van de afscherming van een waal
B. A. De Jong
University of Delft, 1978

[9] Outdoor Sound Propagation Near Ground Surfaces
Karsten Bo Rasmussen
The Acoustics Laboratory, Technical University of Denmark,
Report no. 45 1990

[10] Approximate models for sound propagation above multi-impedance plane boundaries
D. C. Hothersall and J. B. N. Harriot
J. Acoust. Soc. Am. 97, 1995

[11] Prediction of Sound Propagation in a Homogeneous Atmosphere over Flat Terrain with Varying Ground Types
Birger Plovsing
AV 496/97, Delta Acoustics & Vibration, Lyngby, Denmark

[12] Tony Embleton, 1982
Noise Control Engineering, Jan-Feb 1982

[13] Propagation of noise along a finite impedance boundary
C. I. Chessel
J. Acoust. Soc. Am. 62, 1977

[14] A note on the calculation of sound propagation along an impedance boundary
C. F. Chien, W. W. Soroka
J. of Sound and Vibration 69, 1980

[15] On the reflection of a spherical sound wave from an infinite plane
U. Ingard
J. Acoust. Soc. Am. 23, 1951

[15] Acoustic Properties of Fibrous Absorbent Materials
M. E. Delany, E. N. Bazley
Applied Acoustics 3 (2), 1970

# Annex A, Model measurements: Wide screen

The model measurements are described in 4.2 and 5.1.4. In the figure x are measured and — calculated values using the theory in 5.1.2. The position 5 cm from the screen was used as a +6 dB reference, without the screen present, to normalize values relative free field.

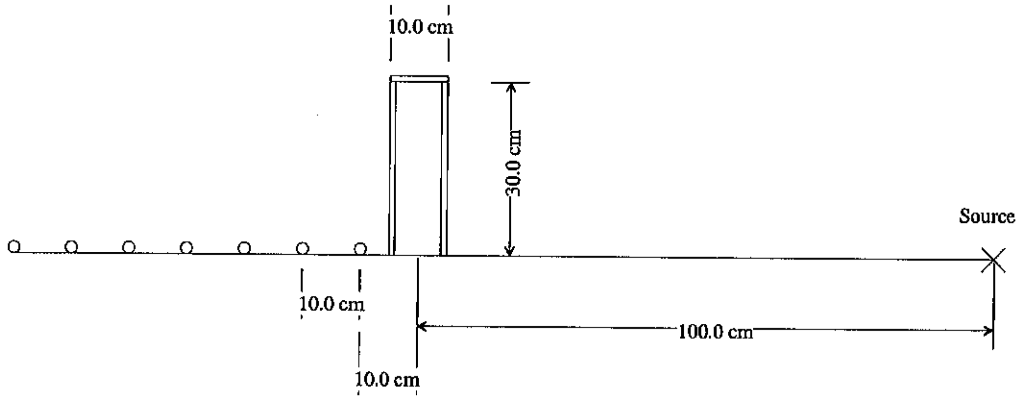


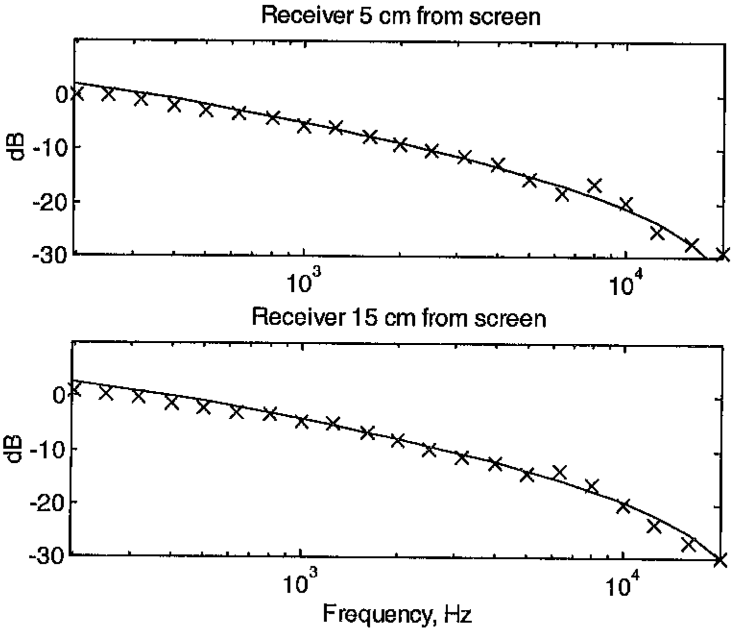

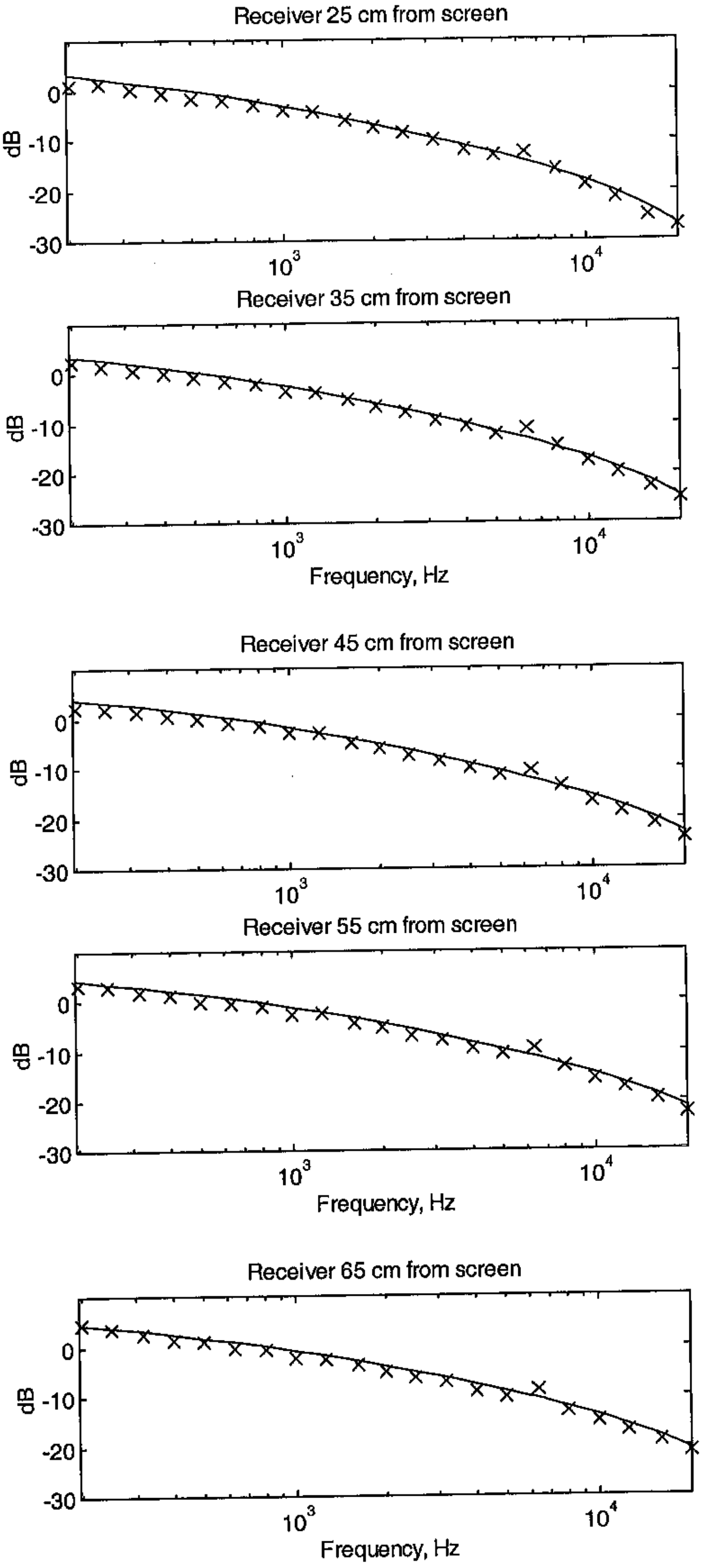
Receiver 25 cm from screen
dB
0
-10
-20
-30
$10^3$
$10^4$
Receiver 35 cm from screen
dB
0
-10
-20
-30
$10^3$
$10^4$
Frequency, Hz
Receiver 45 cm from screen
dB
0
-10
-20
-30
$10^3$
$10^4$
Receiver 55 cm from screen
dB
0
-10
-20
-30
$10^3$
$10^4$
Frequency, Hz
Receiver 65 cm from screen
dB
0
-10
-20
-30
$10^3$
$10^4$
Frequency, Hz

| f(Hz) | 5cm | 15cm | 25cm | 35cm | 45cm | 55cm | 65cm |
|---|---|---|---|---|---|---|---|
| 200 | -0.2 | 0.8 | 1.1 | 2.2 | 2.0 | 3.1 | 4.4 |
| 250 | -0.3 | 0.3 | 1.3 | 1.6 | 1.7 | 3.0 | 3.6 |
| 315 | -1.1 | -0.3 | 0.3 | 0.7 | 1.2 | 1.7 | 2.5 |
| 400 | -2.1 | -1.3 | -0.7 | 0.1 | 0.5 | 1.1 | 1.3 |
| 500 | -2.9 | -2.1 | -1.7 | -0.8 | -0.1 | -0.2 | 1.1 |
| 630 | -3.5 | -2.9 | -2.2 | -1.5 | -1.1 | -0.6 | -0.3 |
| 800 | -4.4 | -3.3 | -3.0 | -2.2 | -1.6 | -1.1 | -0.8 |
| 1000 | -5.8 | -4.6 | -4.1 | -3.5 | -3.0 | -2.8 | -2.3 |
| 1250 | -6.0 | -5.0 | -4.4 | -3.9 | -2.9 | -2.6 | -2.7 |
| 1600 | -7.6 | -6.8 | -6.1 | -5.3 | -4.9 | -4.4 | -3.8 |
| 2000 | -9.1 | -8.1 | -7.6 | -6.8 | -6.0 | -5.3 | -5.3 |
| 2500 | -10.4 | -10.0 | -8.7 | -8.0 | -7.4 | -7.1 | -6.3 |
| 3150 | -11.4 | -11.2 | -10.1 | -9.5 | -8.5 | -7.8 | -7.2 |
| 4000 | -12.9 | -12.4 | -11.9 | -10.8 | -10.1 | -9.5 | -9.1 |
| 5000 | -15.7 | -14.3 | -13.1 | -12.4 | -11.3 | -10.8 | -10.3 |
| 6300 | -18.1 | -13.9 | -12.4 | -11.4 | -10.5 | -9.5 | -9.0 |
| 8000 | -16.6 | -16.3 | -15.9 | -14.7 | -13.8 | -13.2 | -13.1 |
| 10000 | -19.8 | -20.1 | -19.0 | -17.9 | -16.8 | -15.7 | -15.1 |
| 12500 | -25.2 | -23.8 | -21.7 | -20.1 | -18.7 | -17.6 | -17.2 |
| 16000 | -27.5 | -27.0 | -25.1 | -23.0 | -21.2 | -19.9 | -19.1 |
| 20000 | -29.2 | -30.0 | -27.1 | -25.2 | -24.2 | -22.7 | -21.4 |

*Table A.1*
*Model measurements in third octaves. Values normalized to dB rel. free field.*

# Annex B, Model measurements: Double screens

The model measurements are described in 4.2 and 5.2.2. In the figures x are measured and — calculated values using the theory in 5.2. The position 10 cm from the second screen was used as a +6 dB reference, without the screens present, to get values relative free field.

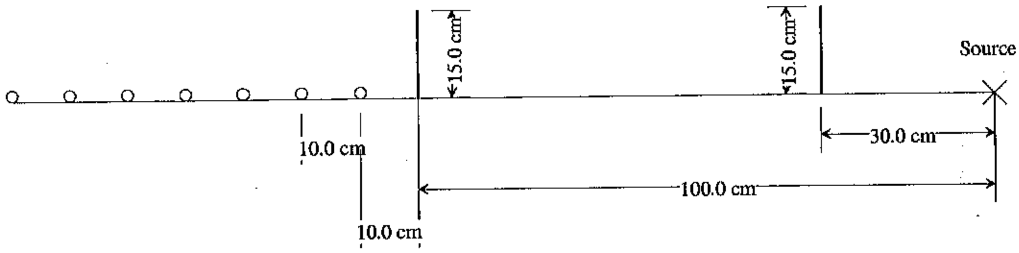


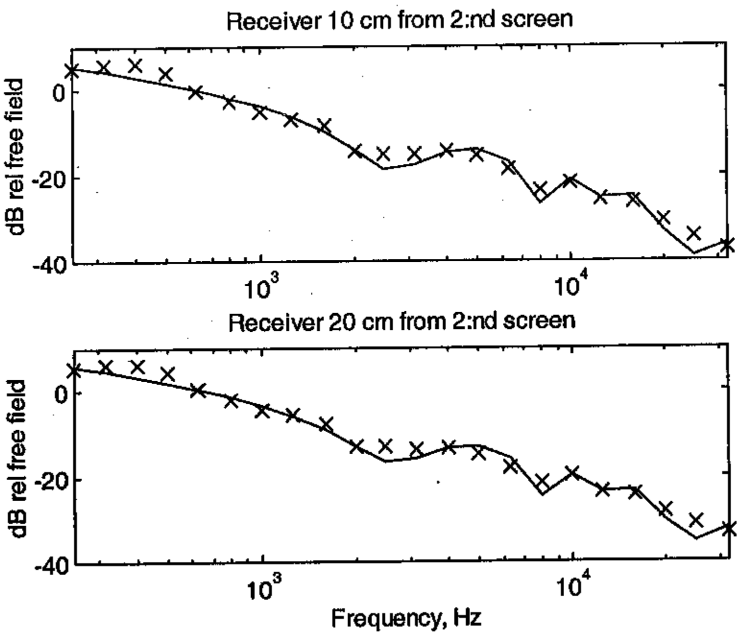


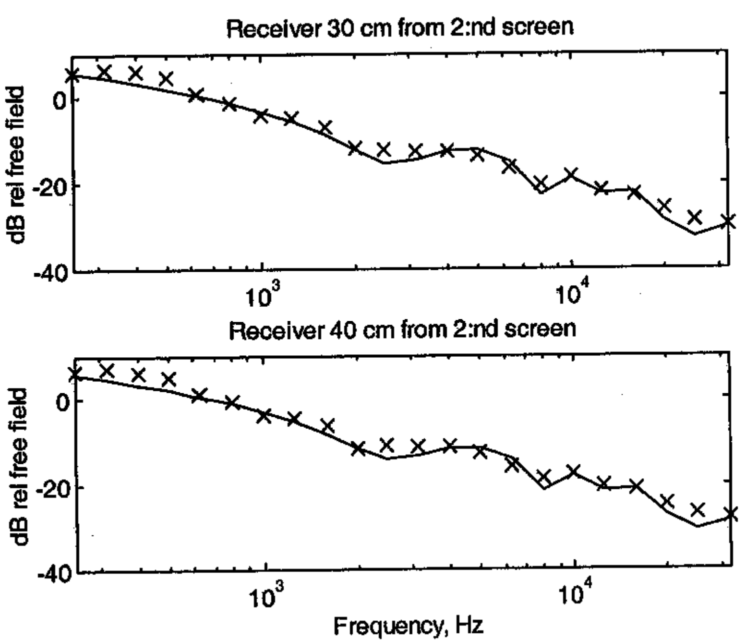

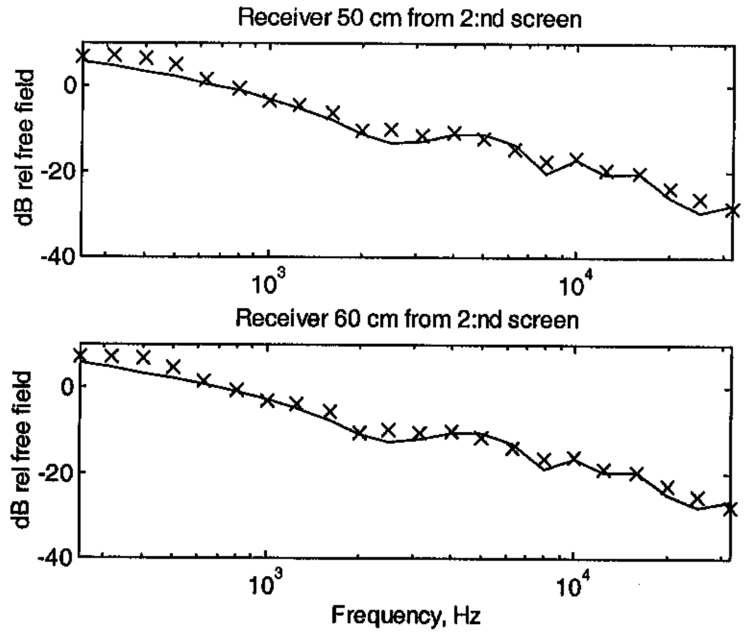


| f(Hz) | 10cm | 20cm | 30cm | 40cm | 50cm | 60cm | 70cm |
|---|---|---|---|---|---|---|---|
| 200 | 4.5 | 5.0 | 5.3 | 4.8 | 5.7 | 6.6 | 6.8 |
| 250 | 5.2 | 5.4 | 5.7 | 6.3 | 6.8 | 7.1 | 7.5 |
| 315 | 5.9 | 6.2 | 6.6 | 7.3 | 7.0 | 7.3 | 7.5 |
| 400 | 6.0 | 6.0 | 6.1 | 6.0 | 6.3 | 6.8 | 6.5 |
| 500 | 4.0 | 4.3 | 4.7 | 5.2 | 4.9 | 4.7 | 5.1 |
| 630 | -0.2 | 0.4 | 0.9 | 1.0 | 1.6 | 1.4 | 1.1 |
| 800 | -2.7 | -2.0 | -1.3 | -0.7 | -0.6 | -0.7 | -0.6 |
| 1000 | -5.1 | -4.6 | -4.1 | -3.7 | -3.4 | -3.2 | -2.6 |
| 1250 | -6.8 | -5.4 | -4.9 | -4.6 | -4.3 | -3.7 | -3.4 |
| 1600 | -8.5 | -7.7 | -6.8 | -6.4 | -6.1 | -5.5 | -5.0 |
| 2000 | -14.5 | -13.0 | -11.9 | -11.6 | -10.5 | -10.5 | -9.6 |
| 2500 | -14.9 | -13.2 | -12.2 | -10.9 | -9.9 | -9.9 | -9.7 |
| 3150 | -14.9 | -13.8 | -12.7 | -11.4 | -11.4 | -10.7 | -9.5 |
| 4000 | -14.2 | -13.5 | -12.4 | -11.4 | -10.7 | -10.2 | -9.6 |
| 5000 | -15.4 | -14.7 | -13.7 | -12.7 | -12.1 | -11.5 | -10.8 |
| 6300 | -18.7 | -17.9 | -16.5 | -16.0 | -14.8 | -14.1 | -13.7 |
| 8000 | -23.4 | -21.4 | -20.1 | -18.7 | -17.3 | -16.6 | -16.2 |
| 10000 | -21.7 | -19.8 | -18.5 | -17.7 | -16.9 | -16.2 | -15.6 |
| 12500 | -25.6 | -23.8 | -21.6 | -20.6 | -19.7 | -19.0 | -18.4 |
| 16000 | -26.4 | -24.4 | -22.6 | -21.3 | -20.4 | -19.7 | -18.5 |
| 20000 | -30.6 | -28.5 | -25.9 | -24.7 | -23.8 | -22.8 | -21.8 |

*Table B.1*
*Model measurements in third octaves. Values normalized to dB rel. free field.*